Effect of submerged small-height obstacle on the dynamics of a distributed heton

Mikhail Sokolovskiy, Jacques Verron, Irina Mickhaylovna Vagina

Effect of a Submerged Small-Height Obstacle on the Dynamics of a Distributed Heton

M. A. Sokolovskiy*, J. Verron, and I. M. Vagina*****

** Institute of Water Problems, Russian Academy of Sciences, ul. Gubkina 3, Moscow, 117735 Russia; e-mail: sokol@aqua.laser.ru*

*** Laboratory of Geophysical and Industrial Flows, National Center of Scientific Research, LEGI, UMR 5519 CNRS, BP 53 X, Grenoble Cedex, 38041 France*

**** Moscow State University, Vorob'evy gory, Moscow, 119899 Russia*

Abstract—In the context of a two-layer quasi-geostrophic model on an *f*-plane, the problem of a self-moving compensated baroclinic vortex (heton) incident on an isolated axially symmetric submerged obstacle of small height is considered. The method of contour dynamics is used to study the characteristic features of the vortex field in the vicinity of the obstacle, depending on the vertical structure of the heton, the height and horizontal sizes of the obstacle, and also the velocity of the background flow.

INTRODUCTION

It is known [1] that the simplest self-moving vortex structure in a plane (stationary or rotating) layer of an unbounded homogeneous fluid is a *system of two rectilinear vortex filaments (point vortices).* In a specific case of a *vortex pair* consisting of two spaced (by some distance r) point vortices with intensities identical in magnitude and opposite in sign, the two vortices move uniformly in straight lines perpendicular to the segment connecting the vortices, and their velocity is proportional to the magnitude of the intensity and inversely proportional to the length of the segment r.[1] In a two-layer fluid [2, 3], a similar pair of vortex filaments belonging to different layers is characterized by a nonmonotonic dependence of the velocity on the distance between the vortices. The velocity of such a two-layer vortex approaches zero at both small and large distances between the vortices and assumes its maximum value at $r = 1.114R_d$, where R_d is the inner Rossby deformation radius [4]. We note that, as a consequence of hydrostatic equilibrium, the vortices of the upper layer with positive (negative) intensity values induce local upward (downward) deformations of the interface, whereas the corresponding deformations induced by the vortices of the lower layer have opposite signs of curvature. Thus, the motion of a pair formed by vortex filaments from different layers is always accompanied by the simultaneous movement of either two ridges or two valleys of the interface. In the case of a stable stratification, the fluid temperature in the upper layer must be higher than that in the lower layer. Therefore, it is evident that, if the interface is deformed upward (downward), the integrated (over the vertical) amount of heat within a vortex tube encircling the vortex filament decreases (increases). Systems consisting of two vortex filaments located in different layers are referred to as *hetons* (derivative of heat) and *antihetons* in the cases when their intensities are opposite and identical in sign, respectively. Hetons with an enhanced (reduced) heat content are called warm (cold) [3, 5].

The concept of heton can be extended to the case of distributed two-layer vortices, when finite-size vortices with constant potential-vorticity values are localized in each of the two layers *(vortex patches).* In this case, in addition to the single dimensionless spatial parameter $l = r/R_d$, which is characteristic of discrete vortices, one more parameter appears: $\gamma = L^*/R_d$, where L^* is the horizontal length scale of the vortex patch. It turns out that, unlike its discrete analogue, a distributed heton can become unstable with respect to small perturbations in its form if $\gamma > 1.7$. In this case, it is able to disintegrate into smaller vortex structures [6–9]. We note a closely related problem of deep convection, in which the heton concept has been successfully used in recent years [10–13]. Specifically, this approach makes it possible to construct physically justified parametrizations of horizontal heat transfer in the ocean, which are necessary for oceanic general circulation models [10].

[1] The intensity of a point vortex is considered to mean the circulation of the velocity induced by this vortex over any closed contour encircling the vortex.

A characteristic property of distributed vortices is also the tendency toward the merging of closely spaced vortex patches identical in the sign of vorticity. Different aspects of the merging of distributed hetons are discussed thoroughly in a number of theoretical [14–22] and experimental [23–25] studies.

On the other hand, little is known about the behavior of vortex pairs located in the vicinity of bottom-topography disturbances [26–28]. This study considers the features of heton motion in the vicinity of an isolated submerged ridge. The objective of the numerical experiments described in this study was to establish the role of the submerged obstacle in the behavior of a baroclinic vortex pair incident on this obstacle. The extent to which the resulting vortex motion is affected by the following factors is revealed: (1) the distance between the centers of the vortex patches forming the heton, (2) the sizes of the vortex patches, (3) the vertical distribution of potential vorticity, (4) the height and horizontal sizes of the submerged ridge, and (5) the velocity of the background flow.

TWO-LAYER MODEL

Let constant values ρ_1 and ρ_2 ($\rho_1 < \rho_2$) be the densities of the upper and lower layers in a two-layer oceanic model and h_1 and h_2 be their arbitrary undisturbed depths, respectively. We introduce a left-handed coordinate system rotating together with the fluid about the vertical z-axis directed downward. Its angular velocity is $f/2$. Thus, in terms of dimensionless variables, we have $z = 0$ at the ocean surface, $z = h_1 - \eta$ at the interface between the layers, and $z = h_1 + h_2 - h \equiv 1 - h$ at the bottom. Further, it is assumed that both the deviation of the interface from its undisturbed state $\eta(x, y, t)$ and the disturbance of the bottom topography $h(x, y)$ are small compared to the total depth of the ocean so that the ratios of their amplitudes to the depth of the ocean are of the order of the Kibel–Rossby number.

It is known [29] that, in the quasi-geostrophic approximation, the following conservation laws are valid provided that the rigid-lid condition is satisfied at the ocean surface and external forcings are absent:

$$\frac{d_i}{dt}\Pi_i = 0, \quad i = 1, 2 \tag{1}$$

where $\mathbf{\Pi}_i$ are the components of the vector of potential vorticity $\mathbf{\Pi}$, which is related to the corresponding vector of pressure anomaly (with respect to the pressure at hydrostatic equilibrium) $\mathbf{p}$ as

$$\mathbf{\Pi} = \nabla^2\mathbf{p} - \gamma^2 A\mathbf{p} + h\mathbf{T}, \quad i = 1, 2. \tag{2}$$

Here, $\gamma^2 = \dfrac{L^{*2}}{R_d^2} = \dfrac{\rho_0 f^2 (h_1 + h_2) L^{*2}}{g\Delta\rho h_1 h_2}$, ρ_0 is the average density of fluid, g is the acceleration of gravity, and $\Delta\rho = \rho_2 - \rho_1$. In addition, the following notation is used in (1) and (2): $\nabla^2 = \dfrac{\partial^2}{\partial x^2} + \dfrac{\partial^2}{\partial y^2}$ and $\dfrac{d_i}{dt} = \dfrac{\partial}{\partial t} + u_i\dfrac{\partial}{\partial x} + v_i\dfrac{\partial}{\partial y}$ for the two-dimensional Laplace operators and the total time derivative, respectively, and also

$$\mathbf{\Pi} = \begin{pmatrix} \Pi_1 \\ \Pi_2 \end{pmatrix}, \quad \mathbf{p} = \begin{pmatrix} p_1 \\ p_2 \end{pmatrix}, \quad \mathbf{T} = \begin{pmatrix} 0 \\ \dfrac{1}{h_2} \end{pmatrix},$$

$$A = \begin{pmatrix} h_2 & -h_2 \\ -h_1 & h_1 \end{pmatrix}.$$

We will treat (2) as a system of differential equations for p_1 and p_2. By separating the variables in (2), we obtain the system of equations

$$h_1\Pi_1 + h_2\Pi_2 - h = \nabla^2\varphi_1, \tag{3}$$

$$\Pi_2 - \Pi_1 - \frac{h}{h_2} = \nabla^2\varphi_2 - \gamma^2\varphi_2 \tag{4}$$

for the new unknown functions

$$\varphi_1 = h_1 p_1 + h_2 p_2, \quad \varphi_2 = p_2 - p_1 \equiv \eta/\mathrm{Fr}, \tag{5}$$

which represent the barotropic stream function and the function describing the behavior of the interface between the layers, respectively. Here, $\mathrm{Fr} = \gamma^2 h_1 h_2$ is the Froude number. We note that the proportionality of the function η to the difference of pressure anomalies in the layers (the second relation in (5)) is obtained by integrating the hydrostatic equation over the vertical with account for the continuity condition satisfied for the total pressure at the surface $z = h_1 - \eta$.

The formal solution of Eqs. (3) and (4) for the desired functions vanishing at infinity can be written in terms of the Green functions of the Laplace and Helmholtz operators (the right-hand sides of Eqs. (3) and (4), respectively) as follows:

$$\varphi_1(x, y, t) = \varphi_{10}(x, y) + \frac{1}{2\pi}\int_{-\infty}^{+\infty}\int_{-\infty}^{+\infty}[h_1\Pi_1(x_1, y_1, t) + h_2\Pi_2(x_1, y_1, t)]\ln R\, dx_1 dy_1, \tag{6}$$

$$\varphi_2(x, y, t) = \varphi_{20}(x, y) + \frac{1}{2\pi}\int_{-\infty}^{+\infty}\int_{-\infty}^{+\infty}[\Pi_2(x_1, y_1, t) - \Pi_1(x_1, y_1, t)]K_0(\gamma R)\, dx_1 dy_1, \tag{7}$$

where $R = \sqrt{(x - x_1)^2 + (y - y_1)^2}$, K_0 is the modified Bessel function[2] and Π_1 and Π_2 obey Eqs. (1). It is evi-

[2] In the following, the modified Bessel functions K_1 and I_0 will also be used with no special explanation.

dent that the time-independent terms φ_{i0} ($i = 1, 2$) must be determined from the equations

$$\nabla^2\varphi_{10} = -h, \tag{8}$$

$$\nabla^2\varphi_{20} - \gamma^2\varphi_{20} = -\frac{h}{h_2}. \tag{9}$$

Additional simplifying assumptions will be formulated in the following section. Here, we determine the parameters h_1 and $\Delta\rho$, which still remain free. We use the method proposed in [30] to construct calibration functionals. According to [30], these potentials lead to the parameters of a two-layer model that correspond optimally to its continuous analogue. In [30], the lower undisturbed boundary of the upper layer (i.e., the average position of the level of density discontinuity) is identified with the level of the peak in the profile of the Brunt–Vaisala frequency squared. This makes it possible to obtain the following simple functional relations:

$$h_1 = \left(\int_0^1 zN^2(z)dz\right)\left(\int_0^1 N^2(z)dz\right)^{-1},$$
$$\Delta\rho = \left(\rho_0\int_0^1 N^2(z)dz\right)g^{-1}. \tag{10}$$

According to formulas (10), the averaged vertical density profiles presented in [29] (Table 1.2.1) give the approximate estimates

$$h_1 = 0.104, \quad \Delta\rho = 3.47\times10^{-3}\rho_0 \text{ and}$$
$$h_1 = 0.095, \quad \Delta\rho = 2.63\times10^{-3}\rho_0$$

for the Pacific and Atlantic oceans, respectively. Thus, setting $h_1 = 0.1$, $\rho_0 = 1$, and $\Delta\rho = 3\times10^{-3}$ in our calculations, we can believe that the model used by us is quite adequate for typical oceanic conditions. We also use the following average values of the main dimensional quantities: $H^* = 4000$ m (the depth of the ocean); i.e., the depths of the upper and lower layers are 400 and 3600 m, respectively; $f = 7.29\times10^{-5}$ s^{-1} (the Coriolis parameter at a latitude of 30°); $U^* = 10$ cm s^{-1} (the characteristic velocity of the orbital motion of particles in a vortex); $g = 980$ cm s^{-2} (the acceleration of gravity). As a result, we estimate the deformation radius at $R_d \approx$ 41.2 km and the Kibel–Rossby number $\varepsilon = U^*/L^*f$ at 0.06 and 0.02 in the cases $\gamma = 1$ and $\gamma = 2.6$ considered below, respectively. These estimates satisfy the conditions of validity of the quasi-geostrophic approximation. The values of the other dimensionless and dimensional quantities are listed below in an individual table.

FORMULATION OF THE PROBLEM OF A HETON INCIDENT ON AN AXIALLY SYMMETRIC SUBMERGED RIDGE

Let the potential vorticity allow the representation

$$\Pi_i = \sum_{j=1}^{n_i}\overline{\Pi}_{ij}(x, y, t), \quad i = 1, 2, \tag{11}$$

where $\overline{\Pi}_{ij}$ are finite functions with finite domains S_{ij} and n_i is the number of vortex patches in the ith layer. Further, let the background field be determined by a zonal current with velocity U and by a topography ridge in the form of a straight circular cylinder with radius a and height h, whose center is located at the origin. In this axially symmetric case, Eqs. (8) and (9) assume the form

$$\frac{1}{r}\frac{d}{dr}\left(r\frac{d\varphi_{10}}{dr}\right) = \begin{cases}-h, & r \le a\\ 0, & r > a,\end{cases} \tag{12}$$

$$\frac{1}{r}\frac{d}{dr}\left(r\frac{d\varphi_{20}}{dr}\right) - \gamma^2\varphi_{20} = \begin{cases}-h/h_2, & r \le a\\ 0, & r > a,\end{cases} \tag{13}$$
$$r = \sqrt{x^2 + y^2}$$

and must be integrated under the conditions

$$\frac{d\varphi_{10}}{dr} \longrightarrow 0, \quad \frac{d\varphi_{20}}{dr} \longrightarrow 0 \quad \text{at} \quad r \longrightarrow \infty, \tag{14}$$

$$\varphi_{10}\big|_{r=a+0} = \varphi_{10}\big|_{r=a-0}, \quad \varphi_{20}\big|_{r=a+0} = \varphi_{20}\big|_{r=a-0}. \tag{15}$$

It is easy to see that the solutions

$$\varphi_{10} = -Uy - \frac{ha^2}{4}\begin{cases}(r/a)^2, & r \le a\\ 1 + 2\ln(r/a), & r > a,\end{cases} \tag{16}$$

$$\varphi_{20} = -\frac{h}{\gamma^2 h_2}\begin{cases}1 - a\gamma I_0(\gamma r)K_1(a\gamma), & r \le a\\ a\gamma I_1(a\gamma)K_0(\gamma r), & r > a,\end{cases} \tag{17}$$

satisfy relations (12)–(15). We note that formula (17) is obtained for φ_{20} by taking into account the known property of the Wronskian $I_n(z)K_{n+1}(z) + I_{n+1}(z)K_n(z) = 1/z$ [32].

If we take into consideration formula (11), we can rewrite relations (6) and (7) as

$$\varphi_1(x, y, t)$$
$$= \varphi_{10}(x, y) + \frac{1}{2\pi}\sum_{i=1}^{2}h_i\sum_{j=1}^{n_i}\overline{\Pi}_{ij}\iint_{S_{ij}(t)}\ln R\,dx_1dy_1,$$

$$\varphi_2(x, y, t)$$

$$= \varphi_{20}(x, y) + \frac{1}{2\pi}\sum_{i=1}^{2}(-1)^i\sum_{j=1}^{n_i}\overline{\Pi}_{ij}\int\int_{S_{ij}(t)}K_0(\gamma R)dx_1dy_1,$$

where the functions φ_{10} and φ_{20} are determined by the solutions given in (16) and (17). Finally, switching to p_1 and p_2 with the use of (5) and expressing the surface integrals in terms of contour integrals by the Stokes formulas, we obtain

$$p_i(x, y, t) = p_{i0}(x, y) + \frac{1}{4\pi}\left\{\sum_{j=1}^{n_i}\overline{\Pi}_{ij}\oint_{C_{ij}(t)}R^2\right.$$

$$\times\left(\ln R - \frac{1}{2}\right)\Theta d\nu_{ij} + h_{3-i}\sum_{m=1}^{2}(-1)^{i+m}\sum_{j=1}^{n_m}\overline{\Pi}_{mj}$$

$$\left.\times\oint_{C_{mj}(t)}\left[\frac{2}{\gamma^2}(\gamma RK_1(\gamma R) - 1) - R^2\left(\ln R - \frac{1}{2}\right)\right]\Theta d\nu_{mj}\right\}, \quad (18)$$

$$i = 1, 2,$$

where C_{ij} are the contours of the domains S_{ij}; $\Theta = [(x_1 - x)\dot{y}_1 - (y_1 - y)\dot{x}_1]/R^2$; p_{i0} are the known functions expressed from (5) in terms of φ_{i0} ($i = 1, 2$); ν_{ij} is a continuous parameter, which is measured counterclockwise and determines the position of the integration variables x_1, y_1 in the jth contour of the ith layer; dots denote differentiation with respect to this parameter.

Formulas (18) show that the pressure and, consequently, the velocities at any point of the plane are completely determined by the configurations of the evolving contours of vortex patches. This result forms the basis for the method of contour dynamics, which was extended in [6] to the case of a two-layer fluid under consideration. The calculation results illustrated below are obtained using the method of contour dynamics. The numerical algorithm used by us is supplemented by the so-called contour surgery procedure [31], which enables us to cut off long and thin vortex filaments and also to remove closely spaced and oppositely oriented portions of the boundaries, i.e., to allow the merging of vortex patches belonging to one layer and having equal potential-vorticity values.

All the above formulas are valid for any finite number of vortex patches in either of the layers n_i ($i = 1, 2$). We will consider the problem of a single heton, i.e., a two-layer vortex, incident on a submerged ridge. We will assume that the condition of vertical compensation

$$h_1\overline{\Pi}_{11} + h_2\overline{\Pi}_{21} = 0, \quad (19)$$

is satisfied for this heton. Moreover, we will assume that motion starts from rest, when the initialization of the current and the generation of the vortex patches forming the heton occur at $t = 0$. It is seen from (3) and (4) that a stationary anticyclonic vortex with the intensity $-h/h_2$ localized in the lower layer corresponds to the time-independent (dependent only on topography) term of the pressure in the field of potential vorticity. For the implementation of rest, a covering cyclonic free vortex with the potential vorticity $\overline{\Pi}_{22} = h/h_2$ should be placed over the ridge at $t = 0$. Thus, in our problem, we have $n_1 = 1$ and $n_2 = 2$ at the initial time.

NUMERICAL RESULTS

First, we indicate the details common to all illustrations. The dimensionless initial radius of all the vortex patches forming the heton is assumed to be equal to unity, and the horizontal spatial scale is always defined as $L^* = \gamma R_d$ if the Rossby deformation radius is specified. We switch to the dimensionless time with the help of the scale multiplier equal to the rotation period of a fluid particle belonging to the heton's contour (initially circular) under the assumption that the lower vortex patch is situated strictly under the upper patch. Actually, the calculation of the time scale always uniquely determines the values of $\overline{\Pi}_{11}$, and $\overline{\Pi}_{21}$, while the value of $\overline{\Pi}_{22}$ depends also on the height of the ridge. We recall that the condition (19) must be satisfied for the heton, and, consequently, the values of $\overline{\Pi}_{i1}$, $i = 1, 2$, are related to each other and depend on the ratio between the depths of the layers.

The initial arrangement of the system of vortices characteristic of all calculation variants and the notation used for the geometrical parameters are given in the first fragment of Fig. 1, where B is the initial distance between the centers of the heton and the submerged ridge and C is the half-distance between the centers of the vortex patches forming the heton. If $C \neq 0$, the heton will be said to have an *inclined axis*. The thick (thin) line depicts the contour of the vortex patch of the upper (lower) layer; the shaded evolving region represents a free vortex, which covers the ridge at the initial time; and the outer boundary of the ridge is marked everywhere by the dashed line.

In the first run of experiments (see Fig. 1), the effect of the value of C—the inclination of the axis of a self-moving heton—on the vortex pattern forming in the vicinity of the ridge is studied. The vortex patches are characterized by the anticyclonic (cyclonic) vorticity in the upper (lower) layer; i.e., the heton is warm.

In Fig. 1a, the process evolves by the following scenario. As the heton approaches the ridge, the free vortex placed over it starts to move and to deform markedly, which favors the manifestation of the anticyclonic rotation of a stationary topographic vortex (initially, this rotation was absent, because the action of topography was completely compensated by the free vortex). It is evident that the effect of the bottom topography is most clearly defined in the lower layer. The cyclonic vortex

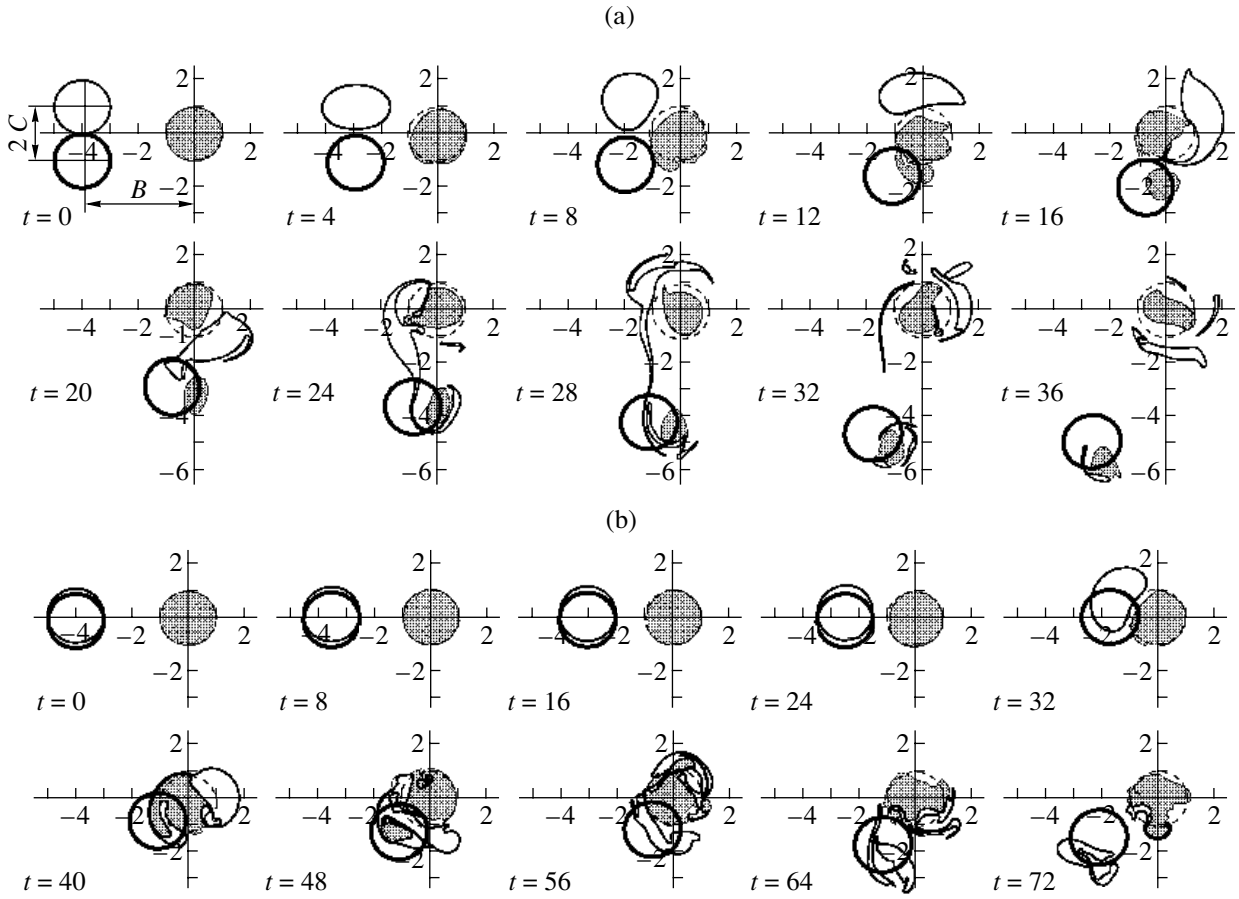

Fig. 1. Evolution of vortex patches in the case of a warm heton incident on a submerged ridge at $h = 1$, $\gamma = 1$, $a = 1$, $B = 4$, and $U = 0$: (a) $C = 1$ and (b) $C = 0.1$.

patch located in this layer is involved in a clockwise rotation and is strongly stretched. On the other hand, the vortex of the upper layer remains essentially undeformed, but this vortex without its "partner" loses the opportunity to execute a further translational motion. At the same time, under the action of the anticyclonic rotation induced by this vortex, a certain part of the free vortex of the lower layer separates and is involved in this rotation: a new self-moving two-layer vortex with an inclined axis is formed. Making a turn around the ridge, the lower-layer cyclone belonging initially to the heton comes under the attraction of the two parts of the free vortex, which results in its partial separation and serves as a cause for its significant degradation. Finally, two configurations are formed: one consists of the parts of two lower-layer cyclones entrained by the topographic vortex and another represents a receding two-layer vortex with an inclined axis. If we disregard the processes occurring at intermediate stages of interaction and compare the configurations at $t = 0$ and $t = 36$, we could infer that the heton falling in the vicinity of the submerged ridge merely changes the direction of its motion. Actually, the structure of its lower part changes radically, because the vortex patch of the lower layer now contains the fluid initially situated over the ridge.

A decrease in the inclination of the heton's axis C by an order of magnitude radically alters the result (see Fig. 1b). Here, the hypothetical situation described in the previous example occurs: making an almost complete turn, a two-layer vortex retains its individuality, although, as in the previous example, the lower-layer cyclone loses a significant portion of vorticity. The point is that the heton is much weaker in this case, because the inclination of its axis is small. As a result, we observe a decrease in the velocity of its motion (this is seen from the indicated times) and, more importantly, the reduction of its effect on the free vortex. Therefore, the larger part of the free vortex remains entrained by the topography and has no way of taking an active part in the interaction with the heton.

In the second run of experiments (see Fig. 2), the features of the formation of the vortex pattern are studied, depending on the vertical distribution of potential vorticity of the incident vortex structure. The cases of warm and cold hetons are considered.

Before we analyze the results of this run, we compare Figs. 1b and 2a. The distinctions between them are

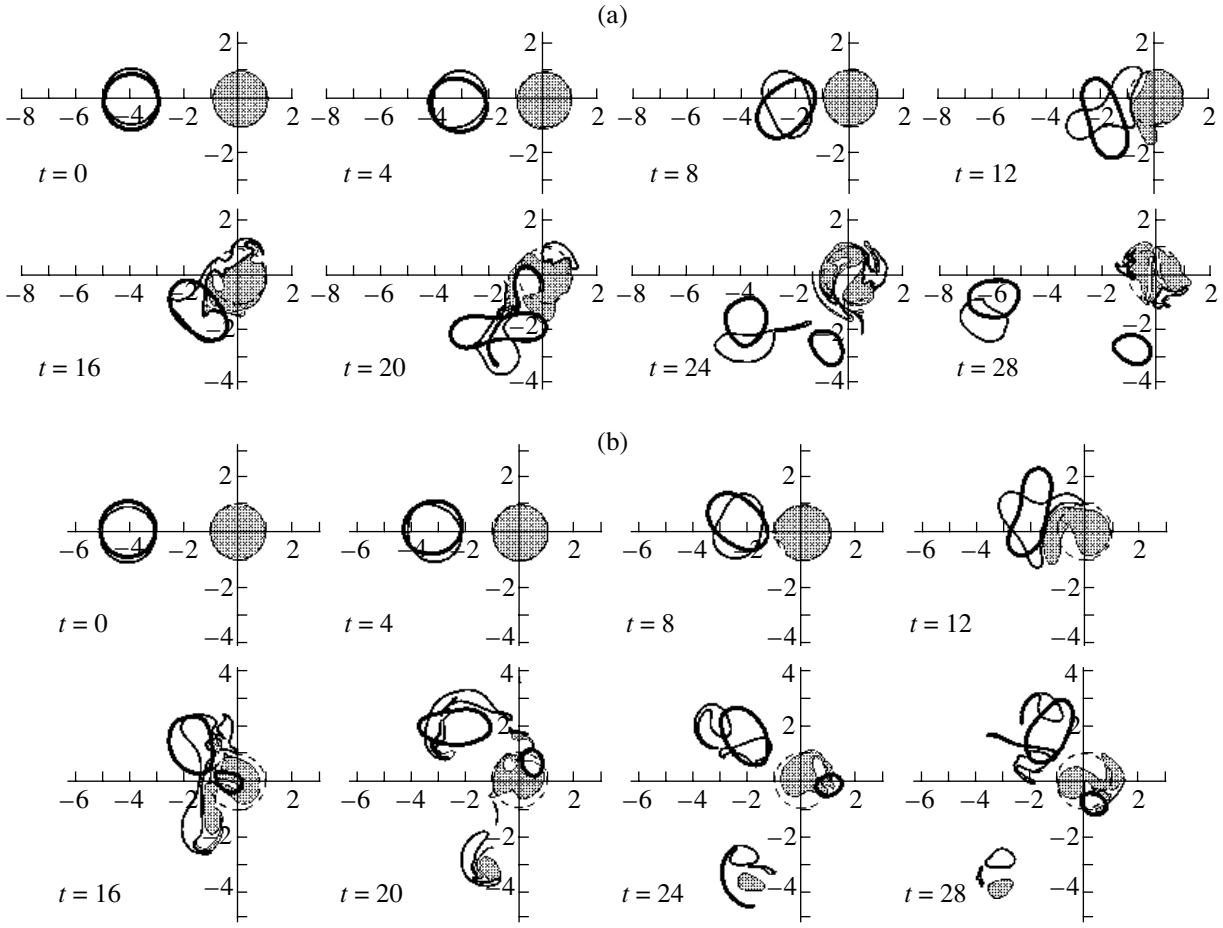

Fig. 2. Evolution of vortex patches in the cases of (a) warm and (b) cold hetons incident on a submerged ridge at $h = 1$, $\gamma = 2.6$, $a = 1$, $B = 4$, $U = 0$, and $C = 0.1$.

due only to different values of the parameter γ. While the initial radii of all vortex patches in the first case are equal to the deformation radius, these radii in the second case are 2.6 times greater than the deformation radius. As was shown in [4], a heton with an inclined axis becomes unstable by itself under these conditions, and it is bound to disintegrate into smaller vortex structures even in the absence of an additional perturbation due to the topography. Especially important here is the fact that the vortex patch of the upper layer also breaks down into two parts, whereas, in Fig. 1, it remains essentially undeformed. Finally, we observe the origination of a new two-layer vortex with opposite rotations in the layers, which consists of parts of the upper-layer and lower-layer vortex patches and moves in the direction nearly opposite to the initial direction; i.e., a kind of inelastic reflection of the heton from the ridge occurs. The remains of the lower-layer vortex patch partially disintegrate and partially merge with the free vortex. The remaining part of the upper-layer vortex patch appears to be located in the vicinity of the ridge for a long time.

The essential difference of the experiment presented in Fig. 2b from all previous experiments is the opposite cyclonic vorticity of either of the vortex patches in the upper and lower layers. Thus, while the interaction between two vortices identical in sign was previously observed in the lower layer, now, the free vortex and the lower vortex of the heton incident on the ridge are opposite in the sign of potential vorticity. In this case, the vortex patches disintegrate in another way. One part of the anticyclone of the lower layer merges with the cyclone separated from the free vortex. The vortex pair so formed in the lower layer leaves the vicinity of the submerged ridge. The cyclonic vortex of the upper layer breaks down into two unequal parts, and the anticyclone of the lower layer breaks down into three parts. The larger part of the upper-layer vortex patch, together with two parts of the lower vortex, forms a two-layer tripolar structure.[3] This structure is sluggish and weakly responds to changes in the topography. At the same time, the smaller part of the upper-layer vortex is

[3] In [4, 7, 14, 15], similar vortex structures were obtained through other mechanisms. It seems likely that one can regard a two-layer tripolar vortex as a rather universal structure.

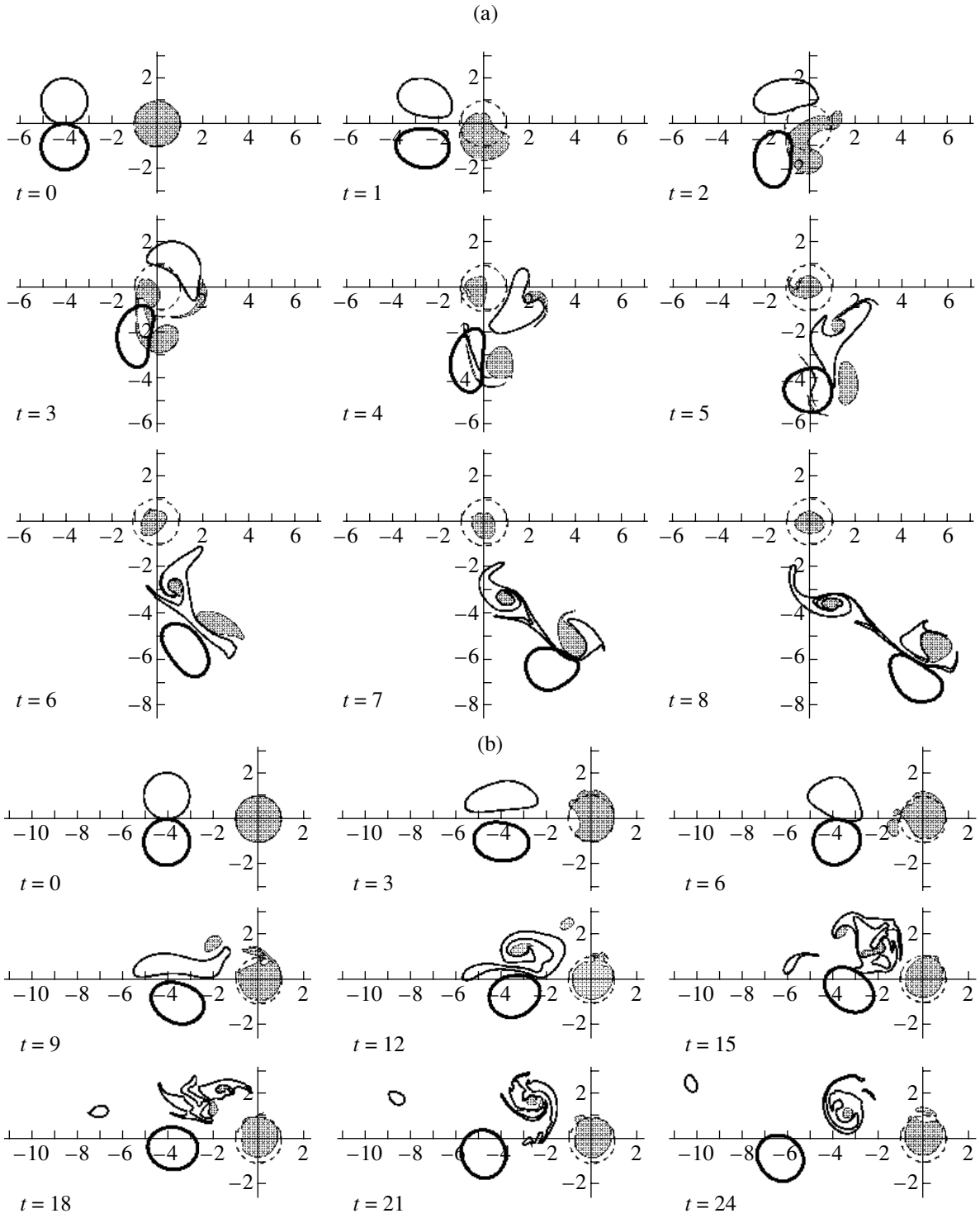

Fig. 3. Evolution of vortex patches in the case of a warm heton incident on a submerged ridge at $h = 2$, $\gamma = 2.6$, $a = 1$, $B = 4$, and $C = 1$: (a) $U = 0.195$ and (b) $U = -0.195$.

entrained in anticyclonic rotation around the ridge. The latter element of vortex motion demonstrates the effect of the topography on the dynamics of the upper layer.

In the next run of experiments (see Fig. 3), the role of an additional external factor—the leading zonal flow—was studied. In addition, the height of the submerged obstacle is increased twofold in these experiments.

In Fig. 3a, the current is in the direction of the proper motion of the two-layer vortex, and the current and heton velocities are equal in magnitude. It is evident that, first, the current must drive the vortex pair

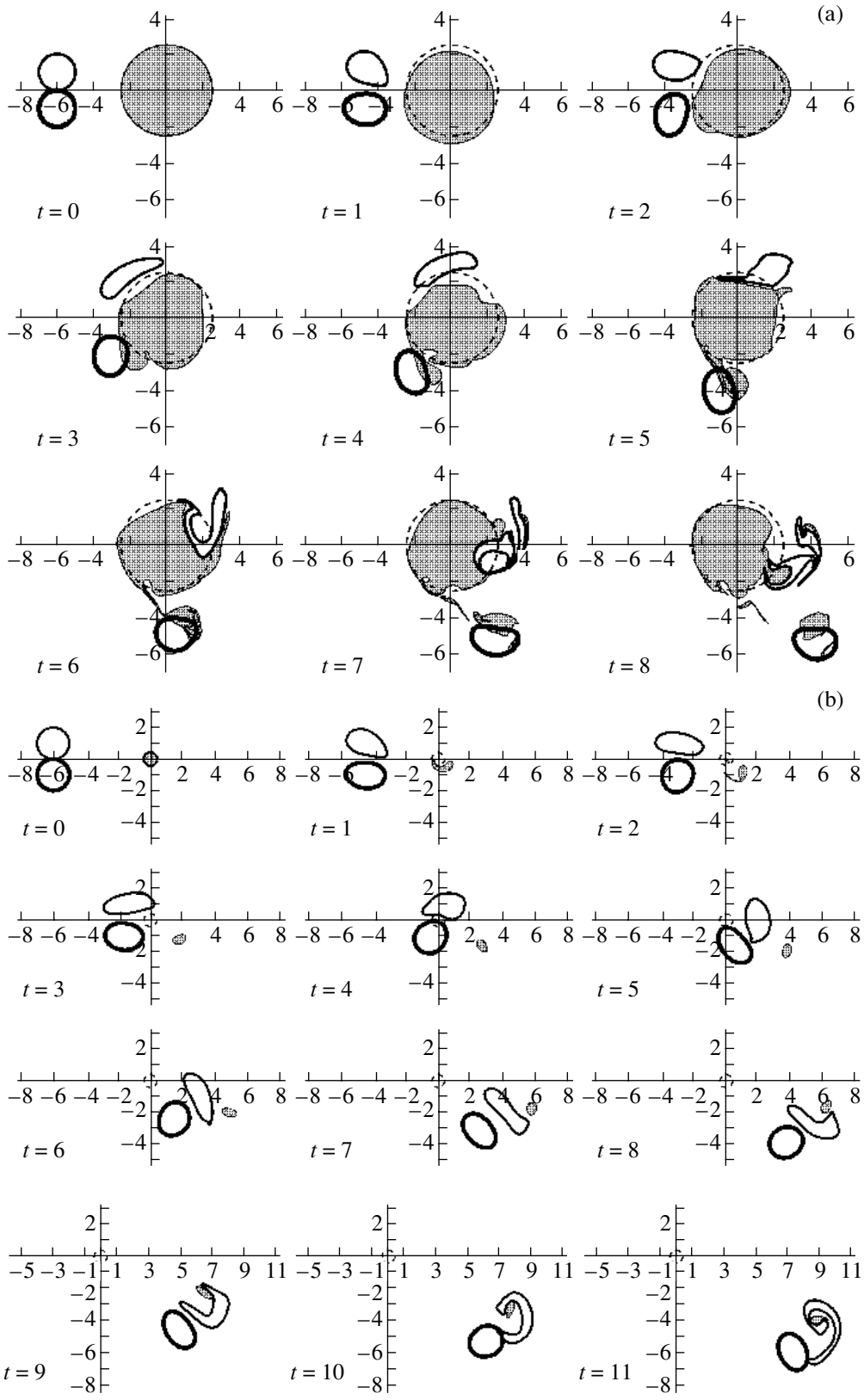

Fig. 4. Evolution of vortex patches in the case of a warm heton incident on a submerged ridge at $h = 2$, $\gamma = 2.6$, $B = 6$, $C = 1$, and $U = 0.195$: (a) $a = 2.5$ and (b) $a = 0.4$.

and, second, it must favor the drift of the free vortex from the ridge. In addition to a purely zonal component, this drift must also have a meridional component due to the deflecting action of the stationary topographic vortex. This situation is observed in the figure. As time passes, the free vortex breaks down into three parts. One part is completely entrained by the topography, and the other two parts merge with two parts of the disintegrated cyclone of the lower layer, respectively. Further, the configuration of the two-layer pair and the cyclonic vortex of the lower layer leaves the vicinity of the ridge, which is favored by the background flow. One part of the free vortex is firmly entrained by the ridge.

In the next experiment of this run (see Fig. 3b), the background current counteracts the motion of the pair, and the heton must occupy a stationary position in the absence of the topography. As is seen from the figure, this situation actually occurs on the time interval $t = 0$–6. Further, the disturbance due to a small part separated from the free vortex by the current starts to manifest itself. A strong interaction between this part (and also a new part separated next from the free vortex) and the cyclonic vortex patch starts to occur. Specifically, this interaction is responsible for the loss of a part of the cyclone. Intraheton interactions weaken, and, as a result, the anticyclone of the upper layer starts to drift under the action of the flow. The tendency toward the drift of the lower-layer vortex patches, which are unaffected by the topography, is also observed. It is believed that the most interesting effect here is the mere fact of the influence of the topography on the heton occupying a stationary position downstream.

Figure 4 demonstrates the effect of the horizontal sizes of the submerged ridge on the formation of a vortex structure in its vicinity. In all previous calculations, the radius of the circular ridge was equal to the initial radii of the vortex patches forming the heton. In Figs. 4a and 4b, this radius is 2.5 times greater and smaller, respectively. The background current is in the direction of heton motion as in Fig. 3a. In the first case, a significant entrainment of both the free vortex and the lower-layer cyclonic vortex initially belonging to the heton is characteristic for a larger size ridge. The two-layer vortex with an inclined axis, which is formed by the upper-layer anticyclone and a part of the free vortex, is carried downstream. In addition, a cyclonic vortex formed from two vortex patches starts to manifest itself in the last fragment shown in the figure. Subsequently, this vortex will also be carried by the current.

A ridge with small horizontal sizes (see Fig. 4b) has little deflecting effect on heton motion. The free vortex is completely carried from the ridge by the current. Then, it merges with the cyclonic vortex and, together with the anticyclone of the upper layer, forms a new two-layer vortex with an inclined axis, which is carried away by the current.

All the figures under consideration only depict evolving configurations of vortex patches. Actually, this is the illustration of fluid motion in the Lagrangian representation, with the only correction that, strictly speaking, the algorithm of the method of contour dynamics does not trace the motion of the individual fluid particles belonging to the boundaries of the vortex patches. In order to improve the approximation properties of the scheme, a uniform redistribution of nodes in each contour occurs at each instant, but all particles belonging to the contour at the initial time stay in this contour.

It is obvious that the more usual Eulerian stream lines give a different pattern of motion, which is confirmed by Fig. 5, where the conditions of the experiment presented in Fig. 3a are repeated. When this approach is used, the role of either of the layers is more clearly defined in the course of their interaction. It is significant that, in the field of stream lines, closed circulation rings are given only by the most intense vortices. Indeed, the condition of vertical compensation (19) imposes the following restriction on the distribution of potential vorticity: $|\overline{\Pi}_{11}| = (h_2/h_1)|\overline{\Pi}_{21}| = 9|\overline{\Pi}_{21}|$; therefore, a rather weak lower-layer vortex patch initially belonging to the heton is almost "unprocessed" here.

The lower row of the figure, where the scale in the "vertical" is significantly exaggerated for clearness, shows that the heton is actually warm and that the stationary anticyclonic vortex of the lower layer induces a local upward deformation of the interface over the ridge.

OCEANOLOGICAL INTERPRETATION OF THE RESULTS

Up to this point, almost nothing has been mentioned about the actual spatial and temporal scales of the processes being modeled. We have indicated only that the total depth of the ocean is assumed equal to 4000 m; the depths of the upper and lower layers are 400 and 3600 m, respectively; and the deformation radius amounts to 41.2 km. The table presented below lists the other external parameters characteristic of the numerical experiments conducted in this work.

We recall that the rotation period, i.e., the time of a complete turn of a fluid particle initially belonging to the circular boundary of the vortex, corresponds to the dimensionless unit of time. Thus, the time intervals corresponding to the processes being modeled usually vary from one and one-half to three years. The exception is Fig. 1b, where the computation time corresponds to about six years.

Of course, the key question remains unanswered as to whether there is reason to believe that heton-type vortices are observed in the ocean. We are unaware of any evidence to support the existence of such structures, as we are unaware of detailed instrumental measurements of the vertical structure of an individual vortex. Nevertheless, one can support the existence of vortices rotating in opposite directions at the upper and lower horizons. V.M. Gryanik[4] proposes the following

[4] Private communication.

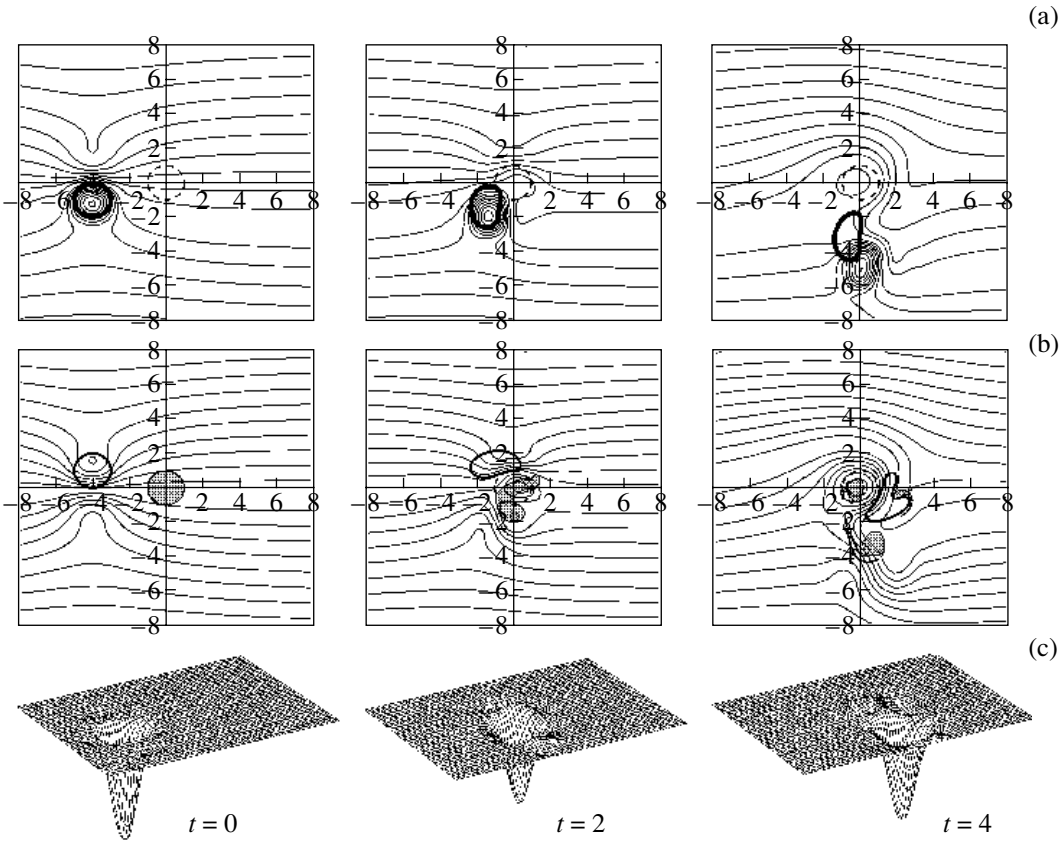

Fig. 5. Stream lines of horizontal motion with superimposed configurations of vortex patches in the (a) upper and (b) lower layers and (c) isometric projections of the interface between the layers at the dimensionless time instants indicated ($h = 2$, $\gamma = 2.6$, $a = 1$, $B = 4$, $C = 1$, $U = 0.195$).

possible mechanism of their formation. In the autumn–winter period of ocean surface cooling, very intense convective motions due to the descent of cold surface waters are observed. It is evident that these waters do not reach the bottom, but they attain the level at which they meet colder underlying water masses; i.e., a clearly defined two-layer structure is formed. It is also obvious that the convective motions cannot be horizontally uniform. Most likely, extended patches encompassing closed domains of the upper layer, where the process is most intense, must be observed. Within each domain, the naturally arising interface must have a downward deformation in its central part. Consequently, in view of the above considerations, an anticyclonic (cyclonic) circulation must arise in the upper (lower) layer; i.e., a warm heton is formed. Because of their sluggishness, these vortex motions can have a time scale significantly greater than the period of the convective motions generated them.

Table

Figure	Dimensionless parameters					Dimensional quantities				
	γ	ε	a	h	U	vortex radius, km	ridge radius, km	ridge height, m	rotation period, days	current velocity, cm/s
1	1	0.06	1	1	0	41.2	41.2	228	29.3	0
2	2.6	0.02	1	1	0	107.2	107.2	228	76.1	0
3a	2.6	0.02	1	2	0.195	107.2	107.2	456	76.1	1.95
3b	2.6	0.02	1	2	−0.195	107.2	107.2	456	76.1	−1.95
4a	2.6	0.02	2.5	2	0.195	107.2	268.0	456	76.1	1.95
4b	2.6	0.02	0.4	2	0.195	107.2	42.9	456	76.1	1.95
5	2.6	0.02	1	2	0.195	107.2	107.2	456	76.1	1.95

If this scheme is plausible, it can be used as the basis for a possible mechanism of heton formation in the ocean.

MAIN RESULTS

The numerical experiments carried out in this work make it possible to establish some features in the formation of the vortex structure in the vicinity of an isolated submerged ridge when a heton with an inclined axis is incident on it. Specifically, the following results are obtained.

If the horizontal sizes of the ridge are of the order of the average vortex radius, even a small (in height) perturbation in the bottom topography significantly deflects the trajectory of the initial motion of a two-layer vortex (Fig. 1). The direction of motion can change and even be reversed. The ridge with a small radius has little deflecting effect on heton motion.

The greatest vortex activity is observed within the lower layer, where a strong interaction occurs among the lower vortex patch of the heton, the free vortex, and the stationary topographic vortex. Due to the fact that closely spaced vortex patches belonging to the same layer and having the same sign tend to merge, water masses are frequently redistributed so that the vertical structure of two-layer vortices changes significantly. If vortex patches of different signs are localized in the lower layer, their interaction has quite a different character. Therefore, warm and cold hetons are affected quite differently by the ridge. For example, the experiment demonstrated in Fig. 2 shows that, after an active interaction between a warm (cold) heton and a submerged obstacle, a two-layer vortex with an inclined axis (a pair formed by two lower-layer patches opposite in the sign of vorticity) moves away from the obstacle.

The horizontal sizes of a heton or, more specifically, the ratio of the vortex radius to the deformation radius are of great importance. In view of the fact that rather large two-layer vortices are unstable and break down into smaller vortex structures, this also has effect on interactions with the ridge.

We also note the features of the process in which vortices of the same sign approach each other and subsequently merge. As a rule, horizontal mixing is significantly intensified during this process. One vortex starts to break down, radiating *vortex filaments*, whereas the other vortex (*victorious vortex*) remains compact and tends to attract and wind the largest possible part of the first vortex on its core [33]. Manifestations of such an asymmetric interaction can be observed in almost all the figures presented.

In addition to the above qualitative results, we note that this work also shows that the method of contour dynamics is efficient in solving such types of problems. As follows from the illustrations presented, the method of contour dynamics makes it possible to study the evolution of individual vortex structures and to describe the processes of their separation, merging, and reintegration, which is important, for example, in studies of the horizontal mixing of different water masses in the ocean.

ACKNOWLEDGMENTS

The authors are grateful to V.M. Gryanik, V.N. Zyryanov, Z.I. Kizner, G.M. Reznik, and A.N. Vul'fson for their participation in discussions of the results, and also to an anonymous reviewer for helpful remarks.

This work was supported by the Russian Foundation for Basic Research, project no. 98-05-65446, and the INTAS, project no. 94-3614.

REFERENCES

1. Lamb, H., *Hydrodynamics*, Cambridge: Cambridge Univ. Press, 1932, 6th ed. Translated under the title *Gidrodinamika*, Moscow: Gostekhizdat, 1947.
2. Gryanik, V.M., Dynamics of Singular Geostrophic Vortices in a Two-Level Atmospheric (Oceanic) Model, *Izv. Akad. Nauk SSSR, Fiz. Atmos. Okeana*, 1983, vol. 19, no. 3, pp. 227–240.
3. Hogg, N.G. and Stommel, H.M., The Heton, an Elementary Interaction between Discrete Baroclinic Geostrophic Vortices, and Its Implications Concerning Eddy Heat Flow*, Proc. R. Soc. London, A*, 1985, vol. 397, pp. 1–20.
4. Sokolovskiy, M.A. and Verron, J., Finite-Core Hetons: Stability and Interactions, *J. Fluid Mech.*, 2000, vol. 423, pp. 127–154.
5. Hogg, N.G. and Stommel, H.M., Hetonic Explosions: The Breakup and Spread of Warm Pools as Explained by Baroclinic Point Vortices, *J. Atmos. Sci.*, 1985, vol. 48, pp. 1465–1476.
6. Kozlov, V.F., Makarov, V.G., and Sokolovskii, M.A., Numerical Model of the Baroclinic Instability of Axisymmetric Vortices in a Two-Layer Ocean, *Izv. Akad. Nauk SSSR, Fiz. Atmos. Okeana,* 1986, vol. 22, no. 8, pp. 868–874.
7. Carton, X.J. and Correard, S.M., Baroclinic Tripolar Geostrophic Vortices: Formation and Subsequent Evolution, *Proc. IUTAM/SIMFLOW Symp.,* Lyngby, Denmark: Kluwer, 1997.
8. Helfrich, K.R. and Send, U., Finite-Amplitude Evolution of Two-Layer Geostrophic Vortices, *J. Fluid Mech.*, 1988, vol. 197, pp. 331–348.
9. Ikeda, M., Instability and Splitting of Mesoscale Rings Using a Two-Layer Quasi-Geostrophic Model on an *f*-Plane, *J. Phys. Oceanogr.*, 1981, vol. 11, pp. 987–998.
10. Doronina, T., Gryanik, V., Olbers, D., and Warncke, T., A 3D Heton Mechanism of Lateral Spreading in Localized Convection in a Rotating Stratified Fluid, *Alfred Wegener Institut, Berichte aus dem Fachbereich Physik*, 1998, Report no. 87.
11. Jones, H. and Marshall, J., Convection with Rotation in a Neutral Ocean: A Study of Open-Ocean Deep Convection, *J. Phys. Oceanogr.*, 1993, vol. 23, pp. 1009–1039.

12. Legg, S. and Marshall, J., A Heton Model of the Spreading Phase of Open-Ocean Deep Convection, *J. Phys. Oceanogr.*, 1993, vol. 23, pp. 1040–1056.

13. Legg, S., Jones, H., and Vibsteck, M., A Heton Perspective of Baroclinic Eddy Transfer in Localized Open Ocean Deep Convection, *J. Phys. Oceanogr.*, 1996, vol. 26, pp. 2251–2266.

14. Sokolovskiy, M.A., On the Counter Collision of Distributed Hetons, *Dokl. Akad. Nauk SSSR*, 1989, vol. 306, no. 1, pp. 198–202.

15. Sokolovskiy, M.A., Numerical Simulation of the Interaction of Distributed Hetons in a Counter Collision, *Metod konturnoi dinamiki v okeanologicheskikh issledovaniyakh* (Contour Dynamics Method in Oceanological Studies), Vladivostok: Dal'nevost. Otd. Akad. Nauk SSSR, 1990, pp. 40–57.

16. Correard, S.M. and Carton, X.J., Vertical Alignment of Geostrophic Vortices: On the Influence of the Initial Distribution of Potential Vorticity, *Proc. IUTAM/SIMFLOW Symp.*, Lyngby, Denmark: Kluwer, 1997.

17. Polvani, L.M., Zabusky, N.J., and Flierl, G.R., Two-Layer Geostrophic Vortex Dynamics, Part 1. Upper-Layer V-States and Merger, *J. Fluid Mech.*, 1989, vol. 205, pp. 215–242.

18. Polvani, L.M., Two-Layer Geostrophic Vortex Dynamics, Part 2. Alignment and Two-Layer V-States, *J. Fluid Mech.*, 1991, vol. 225, pp. 241–270.

19. Valcke, S. and Verron, J., On Interactions between Two Finite-Core Hetons, *Phys. Fluids A*, 1993, vol. 5, pp. 2058–2060.

20. Valcke, S. and Verron, J., Cyclon–Anticyclon Asymmetry in the Merging Process, *Dyn. Atmos. Oceans*, 1996, vol. 24, pp. 227–236.

21. Valcke, S. and Verron, J., Interaction of Baroclinic Isolated Vortices: The Dominant Effect of Shielding, *J. Phys. Oceanogr.*, 1997, vol. 27, pp. 524–541.

22. Verron, J. and Valcke, S., Scale-Dependent Merging of Baroclinic Vortices, *J. Fluid Mech.*, 1994, vol. 264, pp. 81–106.

23. Griffiths, R.W. and Hopfinger, E.J., Experiments with Baroclinic Vortex Pairs in a Rotating Fluid, *J. Fluid Mech.*, 1986, vol. 173, pp. 501–518.

24. Griffiths, R.W. and Hopfinger, E.J., Coalescing of Geostrophic Vortices, *J. Fluid Mech.*, 1987, vol. 178, pp. 73–97.

25. Nof, D. and Simon, L.M., Laboratory Experiments on the Merging of Nonlinear Anticyclonic Eddies, *J. Phys. Oceanogr*, 1987, vol. 17, pp. 343–357.

26. Makarov, V.G., Numerical Modeling of the Effect of Bottom Topography on the Dynamics of a Pair of Quasi-Geostrophic Vortices in a Homogeneous Ocean, *Preprint of Pacific Inst. of Oceanology, Far East Div., USSR Acad. Sci.*, Vladivostok, 1986.

27. Kloosterziel, R.C., Carnevale, G.F., and Philippe, D., Propagation of Barotropic Dipoles over Topography in a Rotating Tank, *Dyn. Atmos. Oceans*, 1993, vol. 19, pp. 65–100.

28. Smith IV, D.C. and O'Brien, J.J., The Interaction of a Two-Layer Isolated Mesoscale Eddy with Bottom Topography, *J. Phys. Oceanogr.*, 1983, vol. 13, pp. 1681–1697.

29. Kamenkovich, V.M., Koshlyakov, M.N., and Monin, A.S., *Sinopticheskie vikhri v okeane* (Synoptic Vortices in the Ocean), Leningrad: Gidrometeoizdat, 1987.

30. Flierl, G.R., Models of Vertical Structure and the Calibration of Two-Layer Models, *Dyn. Atmos. Oceans,* 1978, vol. 2, pp. 341–381.

31. Makarov, V.G., Computational Algorithm of the Method of Contour Dynamics with Varying Topology of the Domains under Study, *Model. Mekh.*, 1991, vol. 5(22), no. 4, pp. 83–95.

32. *Handbook of Mathematical Functions*, Abramowitz, A. and Stegun, I., Eds., New York: Dover, 1971. Translated under the title *Spravochnik po spetsial'nym funktsiyam,* Moscow: Nauka, 1979.

33. Melander, M.V., Zabusky, N.J., and McWilliams, J.C., Asymmetric Vortex Merger in Two Dimensions: Which Vortex Is "Victorious"?, *Phys. Fluids*, 1987, vol. 30, pp. 2610–2612.